Mapping Synergies From Human to Robotic Hands With Dissimilar Kinematics: An Approach in the Object Domain

Guido Gioioso, *Student Member, IEEE*, Gionata Salvietti, *Member, IEEE*, Monica Malvezzi, *Member, IEEE*, and Domenico Prattichizzo, *Member, IEEE*

***Abstract*—One of the major limitations to the use of advanced robotic hands in industries is the complexity of the control system design due to the large number of motors needed to actuate their degrees of freedom. It is our belief that the development of a unified control framework for robotic hands will allow us to extend the use of these devices in many areas. Borrowing the terminology from software engineering, there is a need for middleware solutions to control the robotic hands independently from their specific kinematics and focus only on the manipulation tasks. To simplify and generalize the control of robotic hands, we take inspiration from studies in neuroscience concerning the sensorimotor organization of the human hand. These studies demonstrated that, notwithstanding the complexity of the hand, a few variables are able to account for most of the variance in the patterns of configurations and movements. The reduced set of parameters that humans effectively use to control their hands, which are known in the literature as synergies, can represent the set of words for the unified control language of robotic hands, provided that we solve the problem of mapping human hand synergies to actions of the robotic hands. In this study, we propose a mapping designed in the manipulated object domain in order to ensure a high level of generality with respect to the many dissimilar kinematics of robotic hands. The role of the object is played by a virtual sphere, whose radius and center position change dynamically, and the role of the human hand is played by a hand model referred to as "paradigmatic hand," which is able to capture the idea of synergies in human hands.**

***Index Terms*—Dexterous robotic hands, human skill transfer, robotic grasping, sensory and motor human hand synergies.**

Manuscript received April 2, 2012; revised October 27, 2012; accepted March 7, 2013. Date of publication May 1, 2013; date of current version August 2, 2013. This paper was recommended for publication by Associate Editor T. Simeon and Editor W. K. Chung upon evaluation of the reviewers' comments. This work was supported in part by the European Commission under the Collaborative Project 248587, by "THE Hand Embodied," within the FP7-ICT-2009-4-2-1 program "Cognitive Systems and Robotics," and by the Collaborative EU-Project "Hands.dvi" in the context of the European Clearing House for Open Robotics Development.

G. Gioioso and D. Prattichizzo are with the Department of Information Engineering and Mathematics, University of Siena, 53100 Siena, Italy, and also with the Department of Advanced Robotics, Istituto Italiano di Tecnologia, 16163 Genova, Italy (e-mail: gioiosog@gmail.com; prattichizzo@ing.unisi.it).

G. Salvietti is with the Department of Advanced Robotics, Istituto Italiano di Tecnologia, 16163 Genova, Italy (e-mail: gionata.salvietti@iit.it).

M. Malvezzi is with the Department of Information Engineering and Mathematics, University of Siena, 53100 Siena, Italy (e-mail: malvezzi@dii.unisi.it).

Color versions of one or more of the figures in this paper are available online at http://ieeexplore.ieee.org.

Digital Object Identifier 10.1109/TRO.2013.2252251

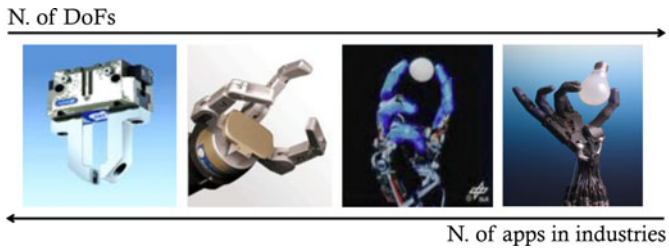

Fig. 1. The larger the number of DoFs of the device, the lower the number of industrial applications where these devices are used.

I. Introduction

A. Motivation and Objective

ROBOTIC hands have many degrees of freedom (DoFs) that are distributed among several kinematic chains: the fingers. The complexity of the mechanical design is needed to adapt hands to the many kinds of tasks required in unstructured environments, such as surgical rooms, industry, house, space, and other domains, where robotic grasping and manipulation have become crucial. Some remarkable examples of a robotic hand design are the UTAH/MIT hand [1] with 16 actuated joints, i.e., four per each finger; the Shadow hand, with 20 actuated joints [2]; and the DLR hand II, with 12 actuated joints [3]. One of the main issues in designing and controlling robotic hands is that a large number of motors are needed to fully actuate the DoFs. This makes both the mechanical and the control system design of robotic hands dramatically more complex when compared with simple grippers that are often used in industrial applications [4], as pictorially represented in Fig. 1: The larger the number of DoFs, the lower the number of possible applications of the robotic hands in industries. This is one of the major limitations to the use of advanced robotic hands in flexible automation, together with the rise of costs and the decrease of the robustness of such devices.

As far as control is concerned, it is our belief that the development of a unified framework for programming and controlling of robotic hands will allow us to extend the use of these devices in many areas. Borrowing the terminology of software engineering, we believe that there is a need for middleware solutions for manipulation and grasping tasks to seamlessly integrate robotic hands in flexible cells and in service robot applications.

This paper is a first contribution in the direction of developing a unified framework for programming and controlling robotic hands based on a number of fundamental primitives,

and abstracting, to the extent possible, from the specifics of their kinematics and mechanical construction. Finally, the ultimate goal of our approach is to define a device-independent control framework for robotic hands, based on synergies of human hands, and this study presents a possible solution to project the synergy-based control of human hands to robotic hands with dissimilar kinematics.

B. Synergies

This paper is inspired and supported by neuroscience studies which have shown that the description of how the human hand performs grasping actions is dominated by postures in a configuration space of much smaller dimension than the kinematic structure would suggest. Such configuration space is referred to as the space of postural synergies. Santello *et al.* [5] investigated this hypothesis by collecting a large set of data that contain grasping poses from subjects that were asked to shape their hands in order to mime grasps for a large set $(N = 57)$ of familiar objects. A principal component analysis (PCA) of these data revealed that the first two principal components account for more than 80% of the variance, suggesting that a satisfying characterization of the recorded data can be obtained using a much lower dimensional subspace of the hand DoF space. These and similar results seem to suggest that, out of the more than 20 DoFs of a human hand, only two or three combinations can be used to shape the hand for basic grasps used in everyday life [6]. These ideas can be brought to use in robotics, since they suggest a new and principled way of simplifying the design and analysis of hands different from other more empirical, sometimes arbitrary design attempts, which has been the main roadblock for research in artificial hands in the past [4]. The application of synergy concepts has been pioneered in robotics by the authors in [7] and [8]. In [7], and later on in [9], the idea has been exploited in the dimensionality reduction of the search space in problems of automated grasp synthesis, and has been applied effectively to derive pregrasp shapes for a number of complex robotic hands. In [8], a robotic hand was designed consisting of groups of mechanically interconnected joints, with a priority inspired by resemblance to postural synergies observed in human hands. More recently, in [10], a synergy impedance controller was derived and implemented on the DLR hand II.

The synergy approach to the analysis and design of artificial hands is the focus of some recent works on grasp theory. In [11], to what extent a hand with many DoFs can exploit postural synergies to control force and motion of the grasped object was investigated. In [12], numerical results were presented that show quantitatively the role played by different synergies (from the most fundamental to those of higher order) in making possible a number of different grasps. In [13], the analysis of underactuated hands was integrated by extending existing manipulability definition [14]–[16]. The main aspect considered there was that in underactuated hands, often the force problem cannot be univocally solved within a rigid-body framework, because of static indeterminacy [11], [12]. This problem can be solved, considering the hand and the contact compliance, as discussed in [17] and [18].

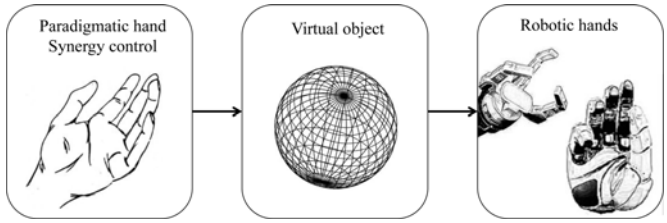

Fig. 2. Mapping between human hand motions and motions of robotic hands with dissimilar kinematics using a virtual object.

C. Mapping

The main contribution of this paper is the study of a mapping function between the postural synergies of the human hand and synergistic control action in robotic devices. This mapping leads to an interesting scenario, where control algorithms are designed, considering a paradigmatic hand model, and without referring to the kinematic of the specific robotic hand. The proposed approach represents a possible control paradigm that has to be used to robustly solve manipulation tasks for parallel jaw grippers that are simple to program but limited in function as well. The *paradigmatic hand* [12], [19] is a model inspired by the human hand that does not closely copy the kinematical and dynamical properties of the human hand, but rather represents a tradeoff between the complexity of the human hand model, accounting for the synergistic organization of the sensorimotor system, and the simplicity and accessibility of the models of the robotic available hands.

This paper focuses on the mapping of human synergies onto robotic hands by using a virtual object method, as shown in Fig. 2. Different mapping procedures have been developed, mainly for tele-manipulation and learning by demonstration tasks. They are summarized in the following section and can be substantially divided in two approaches: joint space and Cartesian space. Both of them are focused on the hand and not on the task. They impose constraints on the choice of the reference joints or points; thus, their applicability to hands with dissimilar kinematics is not intuitive.

The mapping method proposed in this study consists of replicating, on the robotic hand, the effects in terms of motions and deformations that the human reference hand would perform on a virtual object whose geometry is defined by the hand posture itself. This allows us to work directly on the task space, which avoids a specific projection between different kinematics.

This paper is organized as follows. In Section II, a review of the literature, which is related to the mapping between human and robotic hand, is presented. Section III summarizes the main results concerning grasp properties in synergy-actuated hands. Section IV describes the mapping method, while in Section V, some numerical simulations are shown to confirm the proposed approach effectiveness, and the applicability of the method is tested in a manipulation task. Section VI discusses how the proposed mapping procedure can be used to define a two-layer control strategy, in which the high-level controller is substantially independent from the robotic hand, and depends only on the specific operation to be performed. At

the end, in Section VII, the advantages and drawbacks of the proposed method are summarized, and conclusions and future works are outlined.

II. Related Work

In the literature, there are several examples where a mapping between a human hand and a robotic hand is required, and these examples belong usually to two different categories: telemanipulation and learning by demonstration. In the former case, data gloves are typically used to capture human hand motion to move robotic hands. In [20], a DLR hand is controlled using a CyberGlove. In the learning by demonstration case, human data are used to improve the grasping performances by teaching to the robot the correct posture necessary to obtain stable grasps. In [21], human grasps are modeled and evaluated during the arm transportation sequence in order to learn and represent grasp strategies for different robotic hands, while in [22], Do *et al*. proposed a system for vision-based grasp recognition, mapping, and execution on a humanoid robot to provide an intuitive and natural communication channel between humans and humanoids.

Since the kinematics and configuration spaces of a human hand and an artificial robotic hand are typically different, especially when the robotic hand is not anthropomorphic, a mapping function is needed. The main approaches that have been used in the past to deal with this problem are three: joint-to-joint mapping, fingertip mapping, and pose mapping. The first method consists of a direct association between joints on the human hand and joints on the robotic hand. Intuitively, this solution is quite efficient for anthropomorphic hands, while some empirical solutions have to be adopted with nonanthropomorphic devices. An example where joint values of a human hand model are directly used to move joints of a robotic hand can be found in [23]. Although it represents the simplest way to map movements between hands, the joint correspondence mapping is set according to some heuristics, depending on the kinematics of the hands, and it is difficult to generalize the approach to nonanthropomorphic structures.

Cartesian space mappings focus on the relation between the two different workspaces. This solution is more suitable for representing the fingertip positions, and it is a natural approach when, for example, precision grasps are considered. In [24], a point-to-point mapping algorithm is presented for a multifingered telemanipulation system where fingertip motion of the human hand is reproduced with a three-finger robotic gripper. In [25], a virtual finger solution is used to map movements of the human hand onto a four-fingered robotic hand. In [26], a mapping approach, which is divided into three different steps, is proposed. In the first step, a virtual finger approach is used to reduce the number of fingers. Then, an adjustable or gross physical mapping is carried out to get an approximate grasp of the object that is geometrically feasible. Finally, a fine tuning or local adjustment of grasp is performed. Even if this method presents some advantages with respect to the joint-to-joint mapping, it is still not enough general to guarantee a correct mapping in terms of forces and movements exerted by the robotic hand on a grasped object.

The pose mapping can be considered as a particular way of indirect joint angle mapping. The basic idea of pose mapping is to try to establish a correlation between human hand poses and robot hand poses. For example, Pao and Speeter [27] developed an algorithm that tries to translate human hand poses to corresponding robotic hand configurations, without loss of functional information and without the overhead of kinematic calculations, while in [28], neural networks are used to learn the hand grasping posture. Anyway, the proposed solutions under some conditions can produce unpredictable motions of the robot hand and, thus, in our opinion are only exploitable in cases where basic grasp postures are required.

Besides the aforementioned methods, in [29], Griffin *et al.* proposed a 2-D virtual object-based mapping for telemanipulation operations. The object-based scheme assumes that a virtual sphere is held between the thumb of the user and the index finger. Important parameters of the virtual object (the size, position, and orientation) are scaled independently and nonlinearly to create a transformed virtual object in the robotic hand workspace. This modified virtual object is then used to compute the fingertip locations of the robotic hand, which, in this case, is a two-finger, 4-DoFs gripper.

A 3-D extension of the last method is presented in [30]. Even if this extension allows us to analyze more cases, this method is still not enough general for our purposes. In particular, it is constrained by the kinematics of the master and slave hand, the number of contact points (three), and their locations (the fingertips) which have to be the same for both the hands. Then, it can be used only for a given pair of human and robotic hands and for precision grasp operations.

The approach proposed in this paper is inspired by the last two mentioned methods. The main contributions of our work with respect to the methods proposed in [29] and [30] is a generalization to a generic number of contact points that can be different in the human and robotic hands, as well as the removal of constraints on positions of contact points on the master and on the slave hand. We will describe in detail these aspects in the following.

III. Grasp Model and Soft Synergies

This section summarizes the main equations that are necessary to study hands controlled using synergies. Further details on synergies and grasp models can be found in [11] and [31].

Consider a generic hand grasping an object, as sketched in Fig. 3. The hand and the object have n_l contact points. Let $\{N\}$ indicate a reference frame on the hand palm, and $\{B\}$ a reference frame on the object. Let $o \in \Re^3$ denote the position of $\{B\}$ origin with respect to $\{N\}$, and let $\phi \in \Re^3$ denote a vector that describes the relative orientation between the frames (e.g., Euler angles). Furthermore, let $u = [o^{\mathrm{T}} \quad \phi^{\mathrm{T}}]^{\mathrm{T}} \in \Re^6$ collect information on position and orientation between the aforementioned frames.

Compliance can be considered at different levels on the system: The contact between the object and the hand is generally not stiff, and the contact induces a local deformation of the surfaces. Furthermore, the hand links and joint actuators often

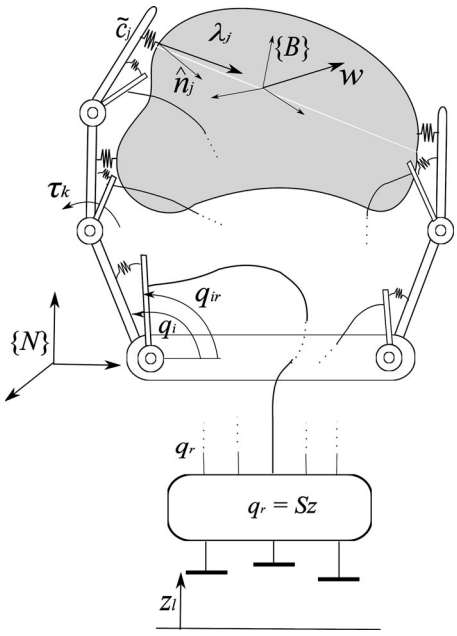

Fig. 3. Main parameters of a synergy-actuated hand with compliant joints and compliant contacts, as defined in [11] and [12].

have compliance levels that have to be considered [32]. In [12], the compliance was introduced at the synergy level as well; however, we did not consider it in this study.

Under a quasi-static condition, the force and moment balance for the object can be described by

$$w = -G\lambda \tag{1}$$

where $w \in \Re^6$ is the external load wrench that is applied to the object, $\lambda \in \Re^{n_c}$ is the contact force vector, and $G \in \Re^{6\times n_c}$ is the grasp matrix. In this paper, for the sake of simplicity, we consider a single point with friction contact model, which is often referred to as a hard finger contact model [31]. With this type of contact model, at each contact point, the force λ_i has three components, and no moments are transmitted. Then, the dimension of the contact force vector λ is $n_c = 3n_l$.

By applying the static–kinematic duality relationship, we can express the velocities $\dot{p}^o \in \Re^{n_c}$ of the contact points on the object as a function of the object twist[1] $\nu^o \in \Re^6$

$$\dot{p}^0 = G^{\mathrm{T}}\nu^o. \tag{2}$$

If a hard finger contact model is assumed, the transpose of the grasp matrix can be expressed as [31]

$$G^{\mathrm{T}} = \begin{bmatrix} I & -[p_1 - o]_\times \\ \cdots & \cdots \\ I & -[p_i - o]_\times \\ \cdots & \cdots \\ I & -[p_{n_l} - o]_\times \end{bmatrix} \tag{3}$$

where $[v]_\times$ refers to the skew matrix that is used to evaluate the cross product of v.

[1] $\nu^o = [\dot{o}^{\mathrm{T}} \quad \omega^{\mathrm{T}}]^{\mathrm{T}}$, where $\dot{o}$ is the object center linear velocity, while ω is the object angular velocity.

Solving (1) for the contact forces introduces the definition of internal forces, i.e., the contact forces included in the nullspace of matrix G. In particular

$$\lambda = -G^{\#}w + A\xi$$

where $G^{\#}$ is the pseudoinverse of the grasp matrix, $A \in \Re^{n_c\times h}$ is a matrix whose columns form a basis for the nullspace of G ($\mathcal{N}(G)$), and $\xi \in \Re^h$ is a vector parameterizing the homogeneous part of the solution to (1). The generic solution of the homogeneous part $\lambda_o = A\xi$ represents a set of contact forces whose resultant force and moment are zero and are referred to as internal forces.

The relationship between hand joint torques $\tau \in \Re^{n_q}$, where n_q is the number of actuated joints, and contact forces is

$$\tau = J^{\mathrm{T}}\lambda \tag{4}$$

where $J \in \Re^{n_c\times nq}$ is the hand Jacobian matrix [31] that relates the contact point velocities on the hand $\dot{p}^h$ to the joint velocities $\dot{q}$

$$\dot{p}^h = J\dot{q}. \tag{5}$$

We suppose that the hand is actuated using a number of inputs whose dimension is lower than the number of hand joints. These inputs are then collected in a vector $z \in \Re^{n_z}$ that parameterizes the hand motions along the synergies.

In this paper, soft synergies, which were previously introduced in [13], are defined as a joint displacement aggregation corresponding to a reduced dimension representation of hand movements, according to a compliant model of joint torques, which can be, for instance, obtained with tendons [33]. In other terms, the reference value of joint angular velocities $\dot{q}_{\mathrm{ref}} \in \Re^{n_q}$ is a linear combination of synergy velocities $\dot{z} \in \Re^{n_z}$ with $n_z \le n_q$

$$\dot{q}_{\mathrm{ref}} = S\dot{z}$$

through the synergy matrix $S \in \Re^{n_q\times n_z}$, whose columns describe the shapes, or directions, of each synergy in the joint space.

As detailed in [11] and [17], to solve the problem of force distribution, we need to introduce other equations, which are usually referred to as constitutive equations, that model the system compliance. Starting from an initial equilibrium condition, the contact force variation is expressed as

$$\Delta\lambda = K_s(J\Delta q - G^{\mathrm{T}}\Delta u) \tag{6}$$

where Δq and Δu are the variations of joint angles and object motion, respectively, and $K_s \in \Re^{n_c\times n_c}$ represents the contact stiffness matrix. If we consider the joint compliance, as discussed, for instance, in [32], the joint torques can also be expressed as

$$\Delta\tau = K_q(\Delta q_{\mathrm{ref}} - \Delta q) \tag{7}$$

where $K_q \in \Re^{n_q\times n_q}$ is the joint stiffness matrix, and Δq_{ref} is the joint reference value variation.

Starting from an equilibrium configuration and applying a small change of the synergy reference value Δz, according to a procedure similar to those described in [17] and detailed

in [11], it is possible to evaluate the corresponding configuration variation. In particular, object displacement Δu is given by

$$\Delta u = V \Delta z \tag{8}$$

where $V = (GKG^{\mathrm{T}})^{-1} GKJS$, in which the equivalent stiffness K is evaluated as $K = (K_s^{-1} + JK_qJ^{\mathrm{T}})^{-1}$ [32]. From (6), one gets the contact force changes $\Delta\lambda$ as

$$\Delta\lambda = P\Delta z \tag{9}$$

where $P = \left(I - G_K^+ G\right) KJS$, with G_K^+ pseudoinverse of grasp matrix G weighted with the stiffness matrix K [17].

For the sake of simplicity, the expressions of matrices P, V, and K summarized here are those obtained by neglecting the so-called geometric effects, arising from the linearization of (4), and depending on J matrix variability with respect to hand and object configuration. A more complete discussion on the role of geometric effects on the grasping linearized equations is presented, for instance, in [34].

Among all the possible motions of the grasped objects, rigid-body motions are relevant since they do not involve viscoelastic deformations in the contact points. Considering (6) and imposing $\Delta\lambda = 0$, the rigid-body motion can be obtained, computing $\mathcal{N}\left[JS - G^{\mathrm{T}}\right]$. Let us then define a matrix Γ, whose columns form a basis of such subspace. Under the hypothesis that the object motion is not indeterminate neither redundant [31], matrix Γ can be expressed as

$$\Gamma = \mathcal{N}\left[\, JS \quad -G^T \,\right] = \begin{bmatrix} \Gamma_{zcs} \\ \Gamma_{ucs} \end{bmatrix} \tag{10}$$

where the image spaces of Γ_{zcs} and Γ_{ucs} consist of coordinated rigid-body motions of the mechanism, for the soft synergy references and the object position and orientation, respectively. It is possible to show that

$$\mathscr{R}(\Gamma_{ucs}) \subseteq \mathscr{R}(V)$$

i.e., rigid-body motions of the object are not all the possible motions of the object controlled by synergies as in (8). The subspace of all synergy-controlled object motions $\mathscr{R}(V)$ also contains motions due to deformations of elastic elements in the model. For a complete discussion on rigid-body motions, including kinematic indeterminacy and redundancy, see [11].

Remark 1: When the free-hand motion is considered, and consequently, the contact forces are zero, according to the compliant model previously introduced in (7), the reference and the actual values of the hand joints are equal, i.e., $q_{\mathrm{ref}} = q$. This assumption is made in Section IV, where the algorithm for mapping synergies of the human hand to robotic hand motions is defined. In Section V, we will analyze the performance of the proposed mapping procedure, both in free-hand motions and during grasping operations. In the latter case, we will use the mapping procedure to command the reference values of the joint variables q_{ref}, which will differ from joint configurations q because of grasping contacts and compliance.

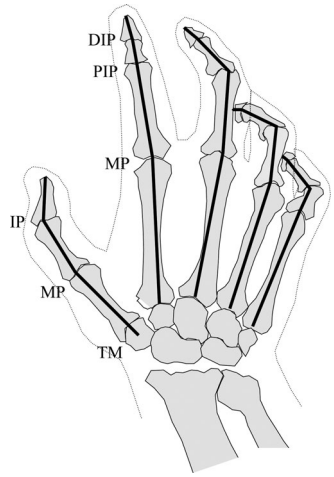

Fig. 4. Scheme of the *paradigmatic* human hand highlighting the joints and the links; the gray dots represent two DoFs joints, while the black dots represent single DoF joints.

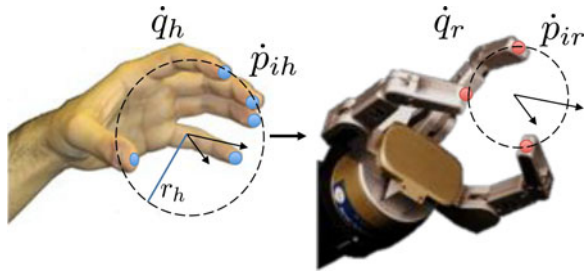

Fig. 5. Mapping synergies from the paradigmatic human hand to the robotic hand. The reference points on the paradigmatic hand p_h (blue dots) allows us to define the virtual sphere. Activating the human hand synergies, the sphere is moved and strained; its motion and strain can be evaluated from the velocities of the reference points $\dot{p}_h$. These motion and strain, scaled by a factor depending on the virtual sphere radii ratio, are then imposed to the virtual sphere relative to the robotic hand, which is defined on the basis of the reference points p_r (red dots).

IV. Mapping Synergies

The target of this study is to define a way to map a set of synergies defined on a reference human hand (the paradigmatic hand shown in Fig. 4) onto a generic robotic hand (see Fig. 5). However, the method can be used to map also arbitrary motions of the human hand, including the case where all the joints are independently controlled.

The kinematic analysis of the paradigmatic hand with postural synergies is reported in [12] and is briefly summarized here. Similar analysis can be found in [35] and [36]. With respect to [12], here, the model has been enriched, adding the distal interphalangeal (DIP) joints for the index, middle, ring, and pinkie fingers, and the abduction/adduction DoF of the middle finger metacarpal joint. The resulting kinematic model has 20 DoFs.

The hand's fingers are modeled as kinematic chains sharing their origin in the hand wrist, as shown in Fig. 4. The bone lengths have been chosen according to the anatomy of the real hand skeleton [37], [38]. The *metacarpophalangeal* (MCP) joint of the index, middle, ring, and pinky fingers has two DoFs each (one for adduction/abduction and another

flexion/extension). The *proximal interphalangeal* (PIP) and DIP joints of the other fingers have one DoF each. The thumb has four DoFs: two DoFs in *trapeziometacarpal* (TM) joint, one DoF in *metacarpophalangeal* (MP) joint, and one DoF in *interphalangeal* (IP) joint.

Let the paradigmatic human hand be described by the joint variable vector $q_h \in \Re^{n_{qh}}$, and assume that the subspace of all configurations can be represented by a lower dimensional input vector $z \in \Re^{n_z}$ (with $n_z \leq n_{qh}$) parameterizing the hand configurations along the synergies, i.e., $q_h = S_h z$, with $S_h \in \Re^{n_{qh} \times n_z}$ being the synergy matrix. In terms of velocities, one gets

$$\dot{q}_h = S_h \dot{z}. \tag{11}$$

Regarding the robotic hand, let $q_r \in \Re^{n_{qr}}$ represent the joint variable vector of the hand. In general, due to the dissimilar kinematics, we can have that the number of joints of the paradigmatic hand differs from that of the robotic hand ($n_{qr} \neq n_{qh}$).

The ultimate goal of this study is to control the reference joint velocities $\dot{q}_r$ of the robotic hand in a synergistic way using the vector of synergies z of the paradigmatic human hand. This is what we mean by kinematic mapping between the human and robotic hands. We want to define the mapping independently from the kinematic structures of the hands, the hand configurations, and the number of possible contact points in case of grasping tasks. To the best of our knowledge, all previous synergy mapping strategies [7], [39] do not explicitly take into account the task to be performed by the robotic hand. In this study, we propose a method of projecting synergies from paradigmatic to robotic hands that explicitly takes into account the task space. To define the mapping, we assume that both the paradigmatic and the robotic hands are in two given initial configurations: q_{0h} and q_{0r} for the human and robotic hands, respectively.

Remark 2: The two initial configurations can be independently chosen. This allows us to obtain a more general mapping procedure, with respect to the methods defined in the configuration space. However, the choice of very dissimilar initial configurations may lead to hand trajectories that appear substantially different in the configuration space, although they produce, on the virtual object, the same displacement and the same deformation. Very dissimilar initial configurations may also lead to other types of problems, for example, one of the hands may reach its joint limits or singular configurations, while the other could move further.

Other than the initial configuration, a set of reference points $p_h = [p_{1h}^{\mathrm{T}}, \ldots, p_{ih}^{\mathrm{T}}, \ldots]^{\mathrm{T}}$ are chosen on the paradigmatic hand. The number of reference points can be chosen arbitrarily.

Remark 3: The reference points can be located on the fingertips or at other points like, for instance, on the intermediate phalanges and/or on the hand palm. Reference points on the fingertips allow us to define the whole hand joint configuration; thus, this is a preferable choice. The role of the reference points is clear when the robotic hand is grasping an object; the reference points correspond to the contact points.

For the paradigmatic hand, the virtual object used to describe the action in the object domain is a virtual sphere, which is computed as the minimum sphere containing the reference points in p_h, as shown in Fig. 5. Note that, in general, not all the points lie on the virtual sphere surface but some of them are contained in it. Let us parameterize the virtual sphere by its center o_h and radius r_h. The motion imposed to the hand reference points by activating the synergies z moves the sphere and deforms it, changing its radius.

In this paper, the motion of the hand due to the synergies is described by modeling the effects of the hand motion on the virtual sphere:

1) a *rigid-body* motion, which is defined by the linear and angular velocities of the sphere center $\dot{o}_h$ and ω_h, respectively;
2) a *nonrigid* strain, which is represented by the radius variation. Let $\dot{r}$ be the radius derivative that the sphere would have if its radius length was 1.

Although the virtual sphere does not represent an object grasped by the paradigmatic hand, it can be easily shown that with a suitable model of joint and contact compliance, the rigid-body motion of the virtual sphere corresponds to the motion of a grasped spherical object and that the nonrigid motion approximately accounts for the normal components of the contact forces for a spherical object grasp.

Representing the motion of the hand through the virtual object, the motion of the generic reference point p_{ih} can be expressed as

$$\dot{p}_{ih} = \dot{o}_h + \omega_h \times (p_{ih} - o_h) + \dot{r}_h (p_{ih} - o_h).$$

Grouping all the reference point motions, one gets

$$\dot{p}_h = A_h \begin{bmatrix} \dot{o}_h \\ \omega_h \\ \dot{r}_h \end{bmatrix} \tag{12}$$

where matrix $A_h \in \Re^{n_{ch} \times 7}$ is defined as follows:

$$A_h = \begin{bmatrix} I & -[p_{1h} - o_h]_\times & (p_{1h} - o_h) \\ \cdots & \cdots & \cdots \\ I & -[p_{ih} - o_h]_\times & (p_{ih} - o_h) \\ \cdots & \cdots & \cdots \end{bmatrix}. \tag{13}$$

It is worth noting that the first six columns of A_h, i.e., its first two column blocks in (13), correspond to the transpose of grasp matrix G, which is defined in (2), and evaluated, considering a hard finger contact model, as shown in (3). Matrix A_h depends on the type of motion that we decide to replicate on the robotic hand, and then, it depends on the task. From (5), (11), and (12), we can evaluate the virtual sphere motion and deformation as a function of the synergy vector velocity $\dot{z}$ of the paradigmatic hand

$$\begin{bmatrix} \dot{o}_h \\ \omega_h \\ \dot{r}_h \end{bmatrix} = A_h^{\#} \dot{p}_h = A_h^{\#} J_h S_h \dot{z} \tag{14}$$

where $A_h^{\#}$ denotes the pseudoinverse of matrix A_h. In this study, we assume that $\mathcal{N}(A_h) = \emptyset$. If this is not the case, virtual sphere motions and/or deformations exist such that the corresponding reference points' displacement is zero. In this case, the problem

is indeterminate, and a unique solution for the mapping problem cannot be identified. This situation is similar to indeterminate grasps, in which the transpose of the grasp matrix has a nontrivial nullspace, as discussed in [31].

Once we modeled the effects of the human hand motion on the virtual sphere motions and deformations, we need to map them on the robotic hand, which is assumed to be in a given initial configuration $q_{0r} \in \Re^{n_{qr}}$ with reference points $p_r \in \Re^{n_{cr}}$. Recall that no hypotheses were imposed on the number of reference points on the paradigmatic human and robotic hands; in general, we can consider $n_{ch} \neq n_{cr}$, neither on their locations, nor on the initial configuration of the two hands.

A virtual sphere is computed in the robotic hand as well. The minimum sphere enclosing the reference points is found, where o_r indicates its center coordinates, and r_r its radius. The virtual spheres within the robotic hand and the human hand can differ in size. Let us define the object scaling factor as the ratio between the two sphere radii

$$k_{\text{sc}} = \frac{r_r}{r_h}. \tag{15}$$

This factor is necessary to scale the velocities from the paradigmatic to the robotic hand workspace. Note that the scaling factor depends on both the size of the hands and on their configurations. Then, the motion and deformation of the virtual sphere generated by the paradigmatic hand are scaled and tracked by the virtual sphere referred to the robotic hand

$$\begin{bmatrix} \dot{o}_r \\ \omega_r \\ \dot{r}_r \end{bmatrix} = K_c \begin{bmatrix} \dot{o}_h \\ \omega_h \\ \dot{r}_h \end{bmatrix} \tag{16}$$

where the scale matrix $K_c \in \Re^{7\times 7}$ is defined as

$$K_c = \begin{bmatrix} k_{\text{sc}} I_{3,3} & 0_{3,3} & 0_{3,1} \\ 0_{3,3} & I_{3,3} & 0_{3,1} \\ 0_{1,3} & 0_{1,3} & 1 \end{bmatrix}.$$

Equation (16) represents the idea at the base of the proposed mapping. What we impose is that the virtual sphere, which is defined on the robotic hand, changes its velocity and radius, according to the sphere that is defined on the paradigmatic hand, apart from the scaling factor.

Following (12) and (13), the corresponding reference point velocity on the robotic hand is given by

$$\dot{p}_r = A_r \begin{bmatrix} \dot{o}_r \\ \omega_r \\ \dot{r}_r \end{bmatrix}$$

where matrix $A_r \in \Re^{n_{cr}\times 7}$ is defined as

$$A_r = \begin{bmatrix} I & -[p_{1r} - o_r]_\times & (p_{1r} - o_r) \\ \cdots & \cdots & \cdots \\ I & -[p_{ir} - o_r]_\times & (p_{ir} - o_r) \\ \cdots & \cdots & \cdots \end{bmatrix}.$$

From (14) and (16), we can express the robotic hand reference point velocities $\dot{p}_r$ as a function of the synergy velocities of the human hand $\dot{z}$ as

$$\dot{p}_r = A_r K_c A_h^{\#} J_h S_h \dot{z}.$$

Finally, considering the robot hand differential kinematics $\dot{p}_r = J_r \dot{q}_r$, where $J_r \in \Re^{n_{cr}\times n_{qr}}$ is its Jacobian matrix, and indicating with $J_r^{\#}$ the robot hand Jacobian pseudoinverse, the following relationship between robot hand joint velocities and synergy velocities can be established

$$\dot{q}_r = J_r^{\#} A_r K_c A_h^{\#} J_h S_h \dot{z}. \tag{17}$$

If the robotic hand in the given grasp configuration is redundant [31], i.e., if $\mathcal{N}(J_r) \neq \emptyset$, the solution of the inverse kinematics problem can be generalized as

$$\dot{q}_r = J_r^{\#} A_r K_c A_h^{\#} J_h S_h \dot{z} + \left(I - J_r^{\#} J_r\right) \zeta$$

where ζ can be arbitrarily set to exploit the redundancy of the robotic hand. The discussion on how to manage the robotic hand redundancy is not explored further in this paper.

Remark 4: The vector of synergies' actuation $\dot{z}$, which is referred to the human hand, is mapped onto the robotic hand joint velocities $\dot{q}_r$ through (17), which is nonlinear and depends on

1) paradigmatic and robotic hand configurations q_{0h} and q_{rh};
2) location of the reference points for the paradigmatic and robotic hands p_h and p_r.

V. Simulations and Performance Analysis

The proposed mapping algorithm was validated through numerical simulations, considering two different robotic hand models. The simulations were carried out using the Syngrasp MATLAB toolbox [40]. The first model was a three-fingered fully actuated robotic hand with the kinematic structure that resembles the Barrett hand [41], with two joints in the thumb (that is fixed with respect to the palm and no abduction/adduction joint) and three joints for each of other two fingers (two flexion/extension and one abduction/adduction). The second model was the DLR/HIT II hand [42]. It has an anthropomorphic structure with five fingers and 15 DoFs. The simulations were performed using MATLAB R2009a over a 2.4-GHz Intel Core i5, 4-GB RAM.

The proposed virtual sphere algorithm was compared with the joint-to-joint mapping and the fingertip mapping methods summarized in Section II. Other mapping methods [29], [30] were not considered since they cannot be extended to kinematic structures that differ from those proposed in the relative papers without introducing heuristic assumptions (e.g., virtual finger). It is worth noting that differently from other approaches where the joint-to-joint mapping only concerns pregrasps [23], we extended its use to grasp analysis including in the hand model both contact and joint compliance. This allows us to easily extend the pure kinematic model to the quasi-static analysis of the grasp.

The actual grasp of different objects was considered. In this analysis, we evaluated what happens if we use the mapping strategy in (17) to control the grasp of real objects. We compared the mapping algorithms in terms of internal force variations and

TABLE I
ENERGY VARIATION ERROR FOR THE BARRETT HAND WITH THREE CONTACT POINTS ON THE PARADIGMATIC HAND

Synergies	Virtual Sphere	Joint-to-joint	Fingertip
Syn 1	21%	62%	122%
Syn 2	10%	192%	103%
Syn 3	50%	30%	166%

TABLE II
ENERGY VARIATION ERROR FOR THE BARRETT HAND WITH FOUR CONTACT POINTS ON THE PARADIGMATIC HAND

Synergies	Virtual Sphere	Joint-to-joint	Fingertip
Syn 1	7%	62%	123%
Syn 2	45%	219%	100%
Syn 3	41%	68%	125%

TABLE III
ENERGY VARIATION ERROR FOR THE DLR-HIT II HAND WITH FOUR CONTACT POINTS (PARADIGMATIC FOUR CONTACT POINTS)

Synergies	Virtual Sphere	Joint-to-joint	Fingertip
Syn 1	12%	87%	86%
Syn 2	54%	244%	103%
Syn 3	52%	83%	73%

TABLE IV
ENERGY VARIATION ERROR FOR THE DLR-HIT II HAND WITH FOUR CONTACT POINTS (PARADIGMATIC THREE CONTACT POINTS)

Synergies	Virtual Sphere	Joint-to-joint	Fingertip
Syn 1	1%	86%	–
Syn 2	26%	211%	–
Syn 3	10%	290%	–

object motions. Both these aspects are fundamental to evaluate the performance of a grasping and manipulation task [43]. In the end, a simulation of a possible application of the method to a manipulation task is reported.

A. Internal Force Evaluation

The proposed mapping method is independent from the number of contact points considered for the paradigmatic and the robotic hands. A direct comparison of the force on the object by the hands is not possible when different number of contact points are selected. We adopted a measure of the whole object deformation produced by the activation of synergies, in a compliant context as described in Section III, to evaluate and compare the performance of the mapping procedure. We considered the energy variation of the hand–object system due to contact forces.

For each mapping method and for each considered robotic hand, a synergy variation Δz was imposed to the paradigmatic human hand resulting into a motion of the robotic hand. Note that the fingers that were not involved in the grasp were moved according to the synergies' activation on the paradigmatic hand, while they were left at their respective initial positions on the robotic hands, for all the simulations. According to (9), the corresponding internal force variation $\Delta\lambda$ was evaluated. Assuming a linear compliant model for the contacts, as those described in (6), the contact force variation corresponds to a deformation of the contact springs. By indicating with Δx the vector containing the deformation components of each contact point, which is evaluated as $\Delta x = K_s^{-1}\Delta\lambda$, the elastic energy variation produced by the activation of synergies can be computed as

$$\Delta E_{el} = \frac{1}{2}K_s\|\Delta x\|^2 = \frac{1}{2}K_s^{-1}\|\Delta\lambda\|^2$$

where K_s is the contact stiffness matrix, which is defined in (6). The sign of the energy variations has been taken into account during the simulations.

Tables I and II show how far the Barrett hand is from replicating the energy obtained with the paradigmatic hand moved along the first, second, and third synergy computed through PCA analysis on experimental measures, as described in [5]. In these simulations, a precision/fingertip grasp is considered. The reported values indicate, in percentage, the energy variation difference. Two cases were considered, with three and four reference points, respectively, on the paradigmatic hand. In both cases, three reference points were assumed on the robotic hand. The size of the grasped object (a real sphere in this case) was selected as to rather fit the average position of the fingers of the paradigmatic hand. The sphere grasped by the Barrett hand was scaled using the scaling factor defined in (16). As can be seen from the tables, energy values that are obtained in the robotic hands using the proposed virtual sphere method are closer to those obtained for the paradigmatic hand, for all the evaluated cases. It is worth to note that when the number of contact points is different, a correction factor $k_{cp} = \frac{n_{ch}}{n_{cr}}$ has to be considered to compare the different values.

Then, deformation energy on the robotic hand was computed as

$$\Delta E_{el,r} = \frac{1}{2}k_{cp}K_s\|\Delta x\|^2.$$

The result trends that are obtained with three and four reference points on the paradigmatic hand are quite similar and show the robustness of the proposed mapping procedure with respect to the number of reference points that are chosen on the paradigmatic hand.

Tables III and IV present the results of similar simulations performed with the DLR-HIT II hand model. We considered the same number of reference points (four) in the robotic hand, while two cases, four and three reference points, respectively, were considered for the paradigmatic hand. In this case as well, the performances of the proposed mapping method are better with respect to other methods, since the energy stored in the contact springs of the robotic hand is closer to the value obtained with the paradigmatic one. This means that the deformation that is imposed to the grasped object by the robotic hand is similar to the deformation that would be impressed by the paradigmatic hand when a certain synergy input variation is applied. Note that, in Table IV, the fingertip method is not considered since, in that example, we considered more fingers in the robotic hand (four) than those considered in the paradigmatic hand (three), and the fingertip method is not directly applicable.

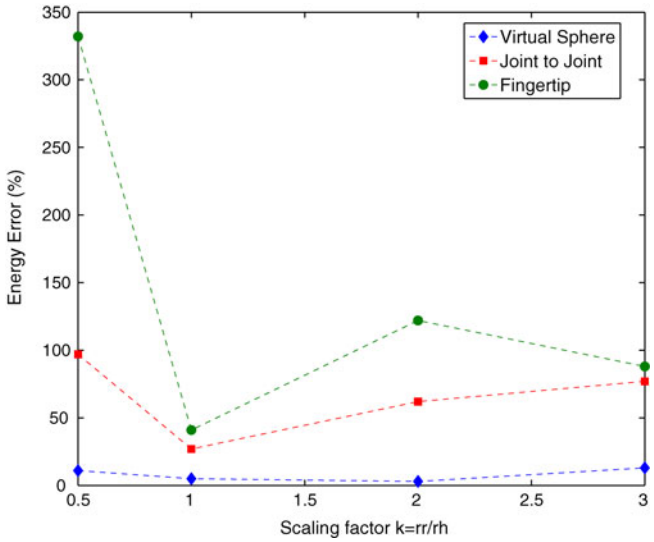

Fig. 6. Energy variation error obtained with the Barrett hand by applying the proposed mapping algorithm, compared with those obtained by applying the joint-to-joint and fingertip mapping methods.

TABLE V
ENERGY VARIATION IN POWER GRASPS

Synergies	Barrett	DLR-HIT
Syn 1	22.27%	19.98%
Syn 2	35.17%	28.22%
Syn 3	53.35%	43.50%

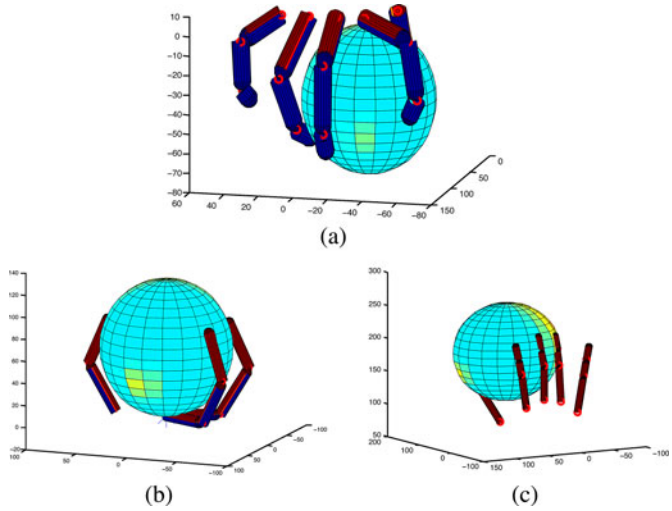

Fig. 7. Power grasp performed by (a) the paradigmatic, (b) the Barrett, and (c) the DLR-HIT II hands.

TABLE VI
ANGULAR DIFFERENCES FOR A CUBE USING THE VIRTUAL SPHERE MAPPING

Synergies	Barrett
Syn 1	27.83°
Syn 2	4.31°
Syn 3	34.85°
Syn 1+2	9.87°
Syn 1+3	1.37°

TABLE VII
ANGULAR DIFFERENCES FOR A CYLINDER USING THE VIRTUAL SPHERE MAPPING

Synergies	DLR-HIT II
Syn 1	18.58°
Syn 2	7.31°
Syn 3	0.92°
Syn 1+2	16.02°
Syn 1+3	16.27°

Additional tests were performed to analyze the sensitivity of the obtained results, in terms of elastic energy variation, with respect to variation of the object size. We considered spheres of different sizes, manipulated by the Barrett hand, driven by the paradigmatic hand grasping always the same sphere. Results obtained by activating only the first synergy are shown in Fig. 6. On the x-axis, the scaling factors computed as the ratio between the two sphere radii are reported. On the y-axis, the elastic energy variation percentage difference between the paradigmatic and the robotic hand is reported. As is clear from the diagram, the virtual sphere algorithm has always a lower difference value, and moreover, its performance is substantially independent from the scaling factor and, thus, from the object size. Similar results are obtained when other synergies are activated.

In Table V, the results for a case of power grasp are presented. Six contact points were considered on the paradigmatic hand, while four and six points were considered on the Barrett and DLR/HIT II hand, respectively. Fig. 7 shows the considered grasps. The better results obtained with the DLR/HIT II hand are due to the highest dexterity of the device that presents 15 DoFs instead of the eight DoFs considered for the Barrett hand.

B. Object Motion During Manipulation

In order to investigate how the mapping procedure influences the grasped object trajectory, we simulated the motion Δu of an object grasped by the robotic hands, while one or a combination of synergies are activated on the paradigmatic hand. As summarized previously, Δu is due both to the rigid-body motions of the hand–object system and to the deformation of the compliance, as seen from the contact points [13]. The vector Δu is composed of the object centroid displacement and object rotation, and was evaluated according to (8). For the sake of simplicity, in the presented results, only the translational component of the object motion was considered. We evaluated the difference between the centroid motion directions of three different objects grasped by the paradigmatic and the robotic hands: a sphere, a cube, and a cylinder. The angular difference was computed, considering the angle between the two motion direction unit vectors on the common spanned plane.

The results for a cubic object motion are reported in Table VI. In this case, we considered the motion due to the activation of the first three synergies separately and combined using the virtual sphere mapping onto the Barrett hand. Concerning the cylinder, Table VII reports the differences between motion directions obtained by mapping, onto the DLR-HIT II hand, the first three synergies, both separately and combined. In Fig. 10, the consider grasps are shown.

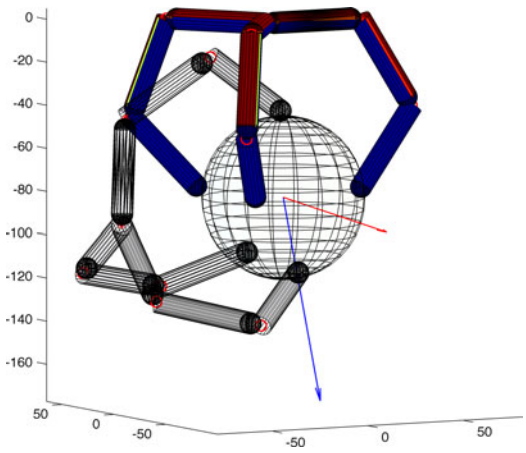

Fig. 8. Barrett hand in two different initial configurations. The blue arrow represents the motion direction, and the red one represents the rotation axis.

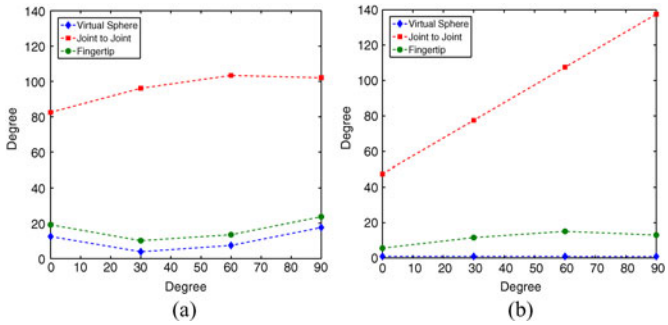

Fig. 9. Angular error of the object motion directions obtained with the three different mapping approaches on (a) the Barrett hand and on (b) the DLR/HIT II hand, with respect to the motion direction of the object manipulated by the Paradigmatic hand.

For the spherical object, we evaluated also the sensitivity of the mapping procedure with respect to hand initial configuration changing the starting position of the robotic hands by varying its palm orientation with respect to the palm of the paradigmatic hand (see Fig. 8). The obtained results are reported in Fig. 9(a) and (b) for the Barrett and the DLR-HIT II hand, respectively.

In the graphs, the angles on the x-axis represent the angular difference between the paradigmatic and robotic palm orientations. The value 0° corresponds to a perfect alignment of the two palms. Then, the orientation was changed by applying to the robotic hand a rotation about a direction taken as normal to the motion direction of the object manipulated by the paradigmatic hand. The obtained results show that the fingertip method and the virtual sphere mapping are substantially independent from the different orientations of the hands. The virtual sphere mapping behaves better in terms of difference between object directions. The joint-to-joint mapping method, instead, obtains worse results, and its sensitivity with respect to hand orientation cannot be disregarded. In particular, in the DLR-HIT II hand, we observe that the joint-to-joint angular error is approximately linearly dependent on the orientation difference between the hands.

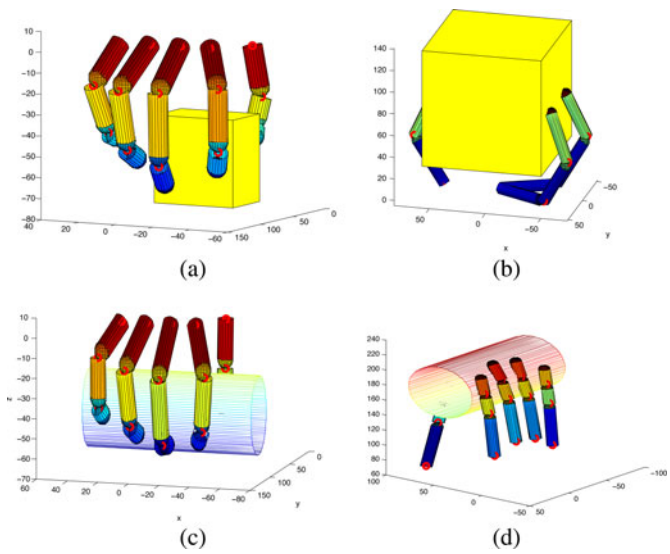

Fig. 10. Manipulation of a cube and a cylinder using Barrett and DLR-HIT II hand, respectively. (a) Paradigmatic hand. (b) Barrett hand. (c) Paradigmatic hand. (d) DLR/HIT II hand.

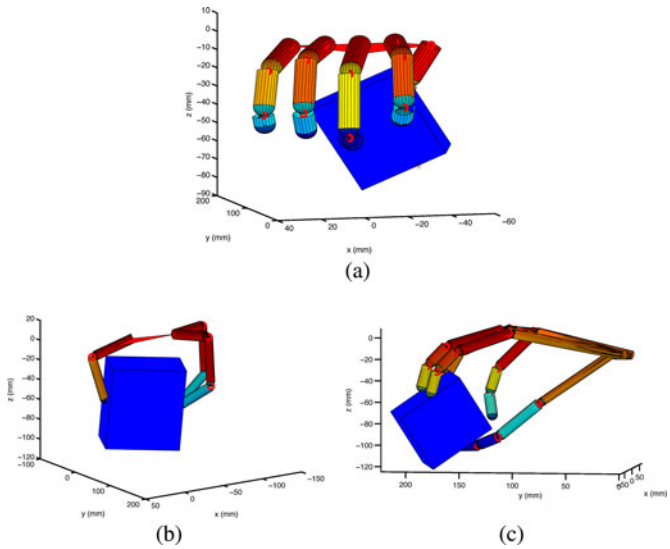

Fig. 11. (a) Human-like hand grasping a cube with the thumb, index, and middle finger; (b) the modular three-finger robotic hand; and (c) the DLR-HIT II hand grasping a cube.

C. Manipulation Task

The mapping algorithm, which was presented in (17), was also tested in a manipulation task. In this example, we considered the grasp of a cubic object. In the initial configuration, the paradigmatic hand grasped the cube with three contact points placed at the fingertips of the thumb, the index finger, and the middle finger, as sketched in Fig. 11(a). We suppose that the internal forces, in the reference configuration, are sufficient to guarantee a stable grasp; then, they satisfy force closure criteria, [31]. The same cube was held by the DLR-HIT II hand, as shown in Fig. 11(c). A cube with dimension increased by a factor 2.5 was grasped by the Barrett hand, as shown in Fig. 11(b). The resulting scaling factor, which is necessary for the virtual sphere mapping algorithm, that depends both on the object size

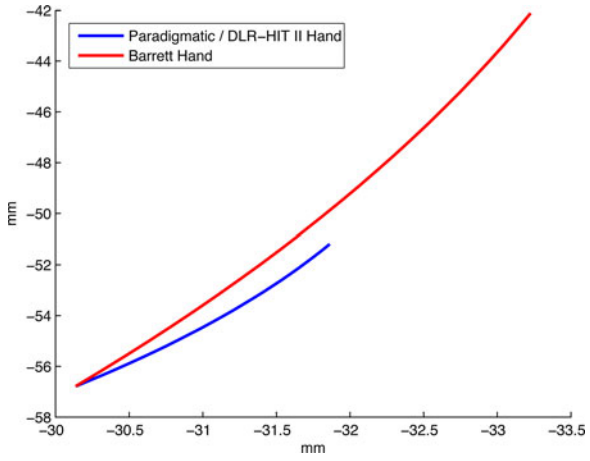

Fig. 12. Trajectories of the cubes manipulated by the paradigmatic hand and the two robotic hands, projected on the X–Z plane of the frame $\{N\}$.

and on the position of the contact points, for the Barrett hand, was $k_{\rm sc} = 2.85$. It is worth recalling that the scaling factor, which is defined in (15), is determined by the configuration of both the robotic and paradigmatic hands once the contact points are fixed.

According to the results presented in [11], when three contact points are considered and a hard finger contact model is assumed, the dimension of the internal force subspace, i.e., the dimension of grasp matrix G nullspace, is three; then, at least a set of four synergies is needed to produce a rigid-body motion, like those defined in (10). The first four synergies for the paradigmatic hand were considered to obtain a rigid-body motion for the object; they were evaluated by calculating matrix Γ in (10). The paradigmatic hand rigid-body motion was then mapped onto movements of the two robotic hands through the proposed virtual sphere mapping algorithm. The centroid of the cube was displaced of 6 mm, along the direction defined by the rigid-body motion imposed by the paradigmatic hand. For each integration step, matrix $\Gamma = [\Gamma_{zcs}^{\rm T} \;\; \Gamma_{ucs}^{\rm T}]$ was evaluated from (10). In this example, $n_z = 4$, $\Gamma_{zcs} \in \Re^4$, and $\Gamma_{ucs} \in \Re^4$; therefore, the rigid-body motion produced by the paradigmatic hand was generated by activating the following synergies $\Delta z = \Gamma_{zcs} \Delta T$, with $\Delta T = 0.04$ s. The corresponding object displacement was $\Delta u_h = \Gamma_{ucs} \Delta T$. The trajectory of the object center can then be updated, and the grasp is evaluated in the new configuration for the paradigmatic hand. For the robotic hands, the object displacements were evaluated according to (8), as $\Delta u_r = V_r \Delta z$. The simulation was carried out in 1.07 s. The trajectories of the cube grasped by the paradigmatic hand and of those manipulated by the robotic hands were then evaluated by numerical integration. For the Barrett hand, the average distance between the final point of the trajectories was 3 mm, and the mean value of the difference, during all the path, was 1 mm. These values have been evaluated taking into account the scaling factor. In the DLR-HIT II hand case, the trajectories were practically the same. The sensibly better performances of the DLR-HIT II hand are a consequence of its higher dexterity with respect to the other one.

In Fig. 12, the trajectories of the cubes manipulated by the three hand models are shown. In this plot, the actual trajectories are displayed without rescaling them to take into account the scaling factor; for this reason, the Barrett hand trajectory is longer than the other two.

VI. Discussion

The proposed mapping strategy, which is based on mimicking behavior of human hand synergies, establishes the foundations of an interface between a higher level control, which defines the synergy reference values z, and the robotic hand. The high level can be thought as independent from the robotic hand structure. The proposed mapping strategy represents the interface, whereby the input synergies are translated into reference joint velocities which actually control the robotic hand. The main advantage of this approach is that the high-level control is substantially independent from the robotic hand and depends only on the specific manipulation tasks to be performed. It can be possible, for example, to use the same controller with different robotic hands or simply substitute a device without changing the controller, thus realizing a sort of abstraction layer for robotic hand control based on synergies. This mapping has been numerically evaluated in grasping and manipulation tasks. Work is in progress to validate the virtual sphere mapping for the approaching phase of grasps as well. Simulation results are encouraging in terms of performances, as shown in the previous section.

However, this approach presents some drawbacks. The proposed mapping is based on a heuristic approach: We choose to reproduce a part of the hand motion, which practically corresponds to move and uniformly squeeze a spherical object. Although uniformly squeezing and moving an object explain a wide range of tasks, many other possibilities exist in manipulating objects, which are not modeled with this mapping. In [44], for instance, an ellipsoid was considered as a virtual object, and its 3-D radial deformation was included in the mapping. The algorithm can be modified to consider different shapes and different types of movements in the task space. Increasing the number of parameters in the virtual object and virtual displacement definition allows us to replicate more complex hand movements but, at the same time, increases the mapping complexity and decreases its robustness.

In this study, we assume that the location of contact points is known. Different grasping planning algorithms (e.g., [45]) can be used to choose the contact points and the hand configurations to be used as parameters of the virtual sphere mapping. Concerning the number of contact points in the paradigmatic and robotic hand, the numerical simulations showed that they influence the performance of the mapping procedure, in terms of object deformation and displacement. For the DLR-HIT II hand, for instance, the best results are obtained when three contact points are considered on the paradigmatic hand, and four points are considered on the robotic one. This is probably due to the fact that the fourth contact point does not add significant information, but on the contrary, it adds a sort of noise in the virtual object displacement and deformation estimation that cannot be replicated by the robotic hand. Furthermore, the different synergies lead to different performance in terms of elastic energy variation and object motions; in particular, the mapping

of synergies that, in the paradigmatic hand, do not produce a significant virtual object displacement or radial deformation is more difficult. This is the case, for example, for the DLR-HIT II hand, of the second synergy and three contact points in the paradigmatic hand, in which the fingers approximately move on the virtual object surface, without producing a significant object displacement or radial deformation.

The performance of the mapping algorithm, in terms of replicating the effect produced by the paradigmatic hand on the object, clearly depends on the kinematic structure of the robotic hand, in particular, on the number of fingers and joints per finger, and their arrangement. Theoretically, there is not a lower bound to the number of fingers and joints to implement the proposed mapping. The minimum level of hand structure complexity can be defined on the basis of the required performance level.

In this paper, we focused on replicating, in terms of virtual object motion and change of internal squeezing force, the action produced by controlling the paradigmatic human hand through synergies. The human hand is the best existing grasping device, and for this reason, we started from it to develop the proposed mapping. In particular, the synergy organization of the hand joint was observed and mapped in this study, since it represents a simple but versatile way to control a complex kinematic structure and, then, is naturally the base on which the mapping procedure was initially developed and tested.

Finally, it is worth underlining that the proposed mapping is not limited to the synergistic motion of the human hand but can be generalized to arbitrary hand motions by simply using, from (11), the joint velocities of the paradigmatic hand in the mapping function (17).

VII. Conclusion and Future Work

Designing synergy-based control strategies in the paradigmatic hand domain can dramatically reduce the dimensionality of the grasping and manipulation problems for robotic hands. However, an efficient mapping is needed to deal with robotic hands with dissimilar kinematics. A synergy-based mapping approach can be useful also under uncertain conditions. The human hand synergies are able to adapt to a wide range of tasks, and to work in uncertain environments, with an almost infinitely wide set of objects. The synergies are defined to synthesize the common components of all these tasks, and then, they represent an optimal tradeoff between simplicity and versatility. A synergy-based mapping can take advantage of these properties and, consequently, can also result in a robust control solution when the environment conditions and/or the planned tasks are uncertain.

We proposed a method for mapping synergies that, using a virtual object, allows us to specify the mappings directly in the task space, thus avoiding the problem of dissimilar kinematics between human-like hand and robotic hands. We compared our solution with the most used solutions existing in the literature, and we evinced that the proposed method is more efficient in terms of internal force mapping and direction of motion. We tested the method in simulation with a two robotic hands' model with dissimilar kinematic structure. Further investigations on different robotic hands are planned. One of the main issue of our approach is that the mapping is not linear and that its implementation may need a high computational burden. The ongoing research is evaluating the conditions, whereby some simplification can be applied to get constant or slowly varying mappings.

References

[1] S. Jacobsen, J. Wood, D. Knutti, and K. Biggers, "The Utah/MIT dextrous hand: Work in progress," *Int. J. Robot. Res.*, vol. 3, no. 4, pp. 21–50, 1984.

[2] The shadow dextrous hand, Shadow Robot Company [Online]. Available: http://www.shadowrobot.com

[3] J. Butterfass, M. Grebenstein, H. Liu, and G. Hirzinger, "DLR-hand II: Next generation of a dextrous robot hand," in *Proc. IEEE Int. Conf. Robot. Autom.*, 2001, vol. 1, pp. 109–114.

[4] A. Bicchi, "Hands for dexterous manipulation and robust grasping: A difficult road toward simplicity," *IEEE Trans. Robot.*, vol. 16, no. 6, pp. 652–662, Dec. 2000.

[5] M. Santello, M. Flanders, and J. Soechting, "Postural hand synergies for tool use," *J. Neurosci.*, vol. 18, no. 23, pp. 10105–10115, 1998.

[6] M. Santello and J. F. Soechting, "Force synergies for multifingered grasping," *Exp. Brain Res.*, vol. 133, no. 4, pp. 457–467, 2000.

[7] M. Ciocarlie, C. Goldfeder, and P. Allen, "Dimensionality reduction for hand-independent dexterous robotic grasping," in *Proc. IEEE/RSJ Int. Conf. Intell. Robot. Syst.*, Oct./Nov. 2007, pp. 3270–3275.

[8] C. Brown and H. Asada, "Inter-finger coordination and postural synergies in robot hands via mechanical implementation of principal components analysis," in *Proc. IEEE/RSJ Int. Conf. Intell. Robot. Syst.*, Oct./Nov. 2007, pp. 2877–2882.

[9] M. Ciocarlie and P. Allen, "Hand posture subspaces for dexterous robotic grasping," *Int. J. Robot. Res.*, vol. 28, pp. 851–867, 2009.

[10] T. Wimboeck, B. Jan, and G. Hirzinger, "Synergy-level impedance control for a multifingered hand," in *Proc. IEEE Int. Conf. Robot. Autom.*, Sep. 2011, pp. 973–979.

[11] D. Prattichizzo, M. Malvezzi, and A. Bicchi, "On motion and force controllability of grasping hands with postural synergies," in *Robotics: Science and Systems VI*. Cambridge, MA, USA: MIT Press, 2010.

[12] M. Gabiccini, A. Bicchi, D. Prattichizzo, and M. Malvezzi, "On the role of hand synergies in the optimal choice of grasping forces," *Auton. Robot.*, vol. 31, pp. 235–252, 2011.

[13] D. Prattichizzo, M. Malvezzi, M. Gabiccini, and A. Bicchi, "On the manipulability ellipsoids of underactuated robotic hands with compliance," *Robot. Auton. Syst.*, vol. 60, no. 3, pp. 337–346, 2012.

[14] J. Salisbury and J. J. Craig, "Articulated hands, force control and kinematic issues," *Int. J. Robot. Res.*, vol. 1, no. 1, pp. 4–17, 1982.

[15] T. Yoshikawa, "Manipulability of robotic mechanisms," *Int. J. Robot. Res.*, vol. 4, no. 2, pp. 3–9, 1985.

[16] A. Bicchi and D. Prattichizzo, "Manipulability of cooperating robots with passive joints," in *Proc. IEEE Int. Conf. Robot. Autom.*, May 1998, vol. 2, pp. 1038–1044.

[17] A. Bicchi, "Force distribution in multiple whole-limb manipulation," in *Proc. IEEE Int. Conf. Robot. Autom.*, May 1993, vol. 2, pp. 196–201.

[18] D. Prattichizzo and A. Bicchi, "Consistent task specification for manipulation systems with general kinematics," *ASME J. Dyn. Syst. Meas. Control*, vol. 119, pp. 760–767, 1997.

[19] G. Baud-Bovy, D. Prattichizzo, and N. Brogi, "Does torque minimization yield a stable human grasp?" in *Multi-Point Physical Interaction with Real and Virtual Objects*, F. Barbagli, D. Prattichizzo, and K. Salisbury, Eds. New York, NY, USA: Springer-Verlag, 2005.

[20] M. Fischer, P. Van der Smagt, and G. Hirzinger, "Learning techniques in a dataglove based telemanipulation system for the DLR hand," in *Proc. IEEE Int. Conf. Robot. Autom.*, May 1998, vol. 2, pp. 1603–1608.

[21] S. Ekvall and D. Kragic, "Interactive grasp learning based on human demonstration," in *Proc. IEEE Int. Conf. Robot. Autom.*, 2004, vol. 4, pp. 3519–3524.

[22] M. Do, J. Romero, H. Kjellstrom, P. Azad, T. Asfour, D. Kragic, and R. Dillmann, "Grasp recognition and mapping on humanoid robots," in *Proc. IEEE/RSJ Int. Conf. Intell. Humanoid Robot.*, Dec. 2009, pp. 465–471.

[23] M. T. Ciocarlie and P. K. Allen, "Hand posture subspaces for dexterous robotic grasping," *Int. J. Robot. Res.*, vol. 28, no. 7, pp. 851–867, 2009.

[24] A. Peer, S. Einenkel, and M. Buss, "Multi-fingered telemanipulation—mapping of a human hand to a three finger gripper," in *Proc. 17th IEEE Int. Symp. Robot. Human Interactive Commun.*, Aug. 2008, pp. 465–470.

[25] J. Liu and Y. Zhang, "Mapping human hand motion to dexterous robotic hand," in *Proc. IEEE Int. Conf. Robot. Biomimet.*, Dec. 2007, pp. 829–834.

[26] S. B. Kang and K. Ikeuchi, "Robot task programming by human demonstration: Mapping human grasps to manipulator grasps," in *Proc. IEEE/RSJ Int. Conf. Intell. Robot. Syst.*, Sep. 1994, vol. 1, pp. 97–104.

[27] L. Pao and T. Speeter, "Transformation of human hand positions for robotic hand control," in *Proc. IEEE Int. Conf. Robot. Autom.*, May 1989, vol. 3, pp. 1758–1763.

[28] P. Gorce and N. Rezzoug, "A method to learn hand grasping posture from noisy sensing information," *Robotica*, vol. 22, no. 3, pp. 309–318, 2004.

[29] W. Griffin, R. Findley, M. Turner, and M. Cutkosky, "Calibration and mapping of a human hand for dexterous telemanipulation," in *Proc. Symp. Haptic Interfaces Virtual Environ. Teleoperator Syst.*, 2000, pp. 1–8.

[30] H. Wang, K. Low, M. Wang, and G. F. , "A mapping method for telemanipulation of the non-anthropomorphic robotic hands with initial experimental validation," in *Proc. IEEE Int. Conf. Robot. Autom.*, Apr. 2005, pp. 4218–4223.

[31] D. Prattichizzo and J. Trinkle, "Grasping," in *Handbook on Robotics,* B. Siciliano and O. Kathib, Eds. New York, NY, USA Springer-Verlag, 2008, pp. 671–700.

[32] S. Chen and I. Kao, "Conservative congruence transformation for joint and Cartesian stiffness matrices of robotic hands and fingers," *Int. J. Robot. Res.*, vol. 19, no. 9, pp. 835–847, 2000.

[33] A. Bicchi and D. Prattichizzo, "Analysis and optimization of tendinous actuation for biomorphically designed robotic systems," *Robotica*, vol. 18, no. 1, pp. 23–31, 2000.

[34] M. Malvezzi and D. Prattichizzo, "Evaluation of grasp stiffness in underactuated compliant hands," in *Proc. IEEE Int. Conf. Robot. Autom.*, 2013, to be published.

[35] S. Cobos, M. Ferre, S. Uran, J. Ortego, and C. Pena, "Efficient human hand kinematics for manipulation tasks," in *Proc. IEEE/RSJ Int. Conf. Intell. Robot. Syst.*, Sep. 2008, pp. 2246–2251.

[36] I. Albrecht, J. Haber, and H. Seidel, "Construction and animation of anatomically based human hand models," in *Proc. ACM SIGGRAPH/Eurograph. Symp. Comput. Anim.*, 2003, pp. 98–109.

[37] S. Mulatto, A. Formaglio, M. Malvezzi, and D. Prattichizzo, "Using postural synergies to animate a low-dimensional hand avatar in haptic simulation," *IEEE Trans. Haptics*, vol. 6, no. 1, pp. 106–116, First Quar., 2013.

[38] K. Kim, Y. Youm, and W. Chung, "Human kinematic factor for haptic manipulation: The wrist to thumb," in *Proc. Symp. Haptic Interfaces Virtual Environ. Teleoperator Syst.*, 2002, pp. 319–326.

[39] T. Geng, M. Lee, and M. Hulse, "Transferring human grasping synergies to a robot," *Mechatronics*, vol. 21, no. 1, pp. 272–284, 2011.

[40] M. Malvezzi, G. Gioioso, G. Salvietti, D. Prattichizzo, and A. Bicchi, "Syngrasp: A MATLAB toolbox for grasp analysis of human and robotic hands," in *Proc. IEEE Int. Conf. Robot. Autom.*, 2013, to be published.

[41] The Barrett hand, Barrett Technologies, Inc., Cambridge, MA, USA [Online], Available: http://www.barrett.com/

[42] J. Butterfass, M. Grebenstein, H. Liu, and G. Hirzinger, "DLR-hand II: Next generation of a dextrous robot hand," in *Proc. IEEE Int. Conf. Robot. Autom.*, 2001, vol. 1, pp. 109–114.

[43] O. Brock, J. Kuffner, and J. Xiao, "Motion for manipulation tasks," in *Handbook on Robotics,* B. Siciliano and O. Kathib, Eds. New York, NY, USA Springer-Verlag, 2008, pp. 615–645.

[44] G. Gioioso, G. Salvietti, M. Malvezzi, and D. Prattichizzo, "An object-based approach to map human hand synergies onto robotic hands with dissimilar kinematics," in *Robotics: Science and Systems VIII*. Cambridge, MA, USA: MIT Press, 2012.

[45] C. Borst, M. Fischer, and G. Hirzinger, "Grasp planning: How to choose a suitable task wrench space," in *Proc. IEEE Int. Conf. Robot. Autom.*, Apr./May 2004, vol. 1, pp. 319–325.

Guido Gioioso (S'13) received the "Laurea Specialistica" (*con Lode*) degree in information engineering from the University of Siena, Siena, Italy, in 2011. He is currently working toward the Ph.D. degree with the Department of Information Engineering and Mathematics, University of Siena, as well as with the Department of Advanced Robotics, Istituto Italiano di Tecnologia, Genova, Italy.

His research interests include robotic and human grasping, haptics, teleoperation, and mobile robots.

Gionata Salvietti (M'12) received the "Laurea Specialistica" (*con Lode*) degree in information engineering with specialization in robotics and automation and the Ph.D. degree in information engineering from the University of Siena, Siena, Italy, in 2009 and 2012, respectively.

He was a Visiting Researcher with the DLR Institute for Robotic and Mechatronics, Wessling, Germany, in 2012 and a Visiting Student with Technical Aspects of Multimodal Systems Group, University of Hamburg, Hamburg, Germany, in 2008. He is currently a Postdoctoral Junior with the Department of Advanced Robotics, Istituto Italiano di Tecnologia, Genova, Italy. His research interests include robotic and human grasping, haptics, and medical robotics.

Monica Malvezzi (M'13) received the Laurea degree in mechanical engineering from the University of Florence, Florence, Italy, in 1999 and the Ph.D. degree in applied mechanics from the University of Bologna, Bologna, Italy, in 2003.

She is an Assistant Professor of mechanics and mechanism theory with the Department of Information Engineering and Mathematics, University of Siena, Siena, Italy. Her main research interests include the control of mechanical systems, robotics, vehicle localization, multibody dynamics, haptics, grasping, and dexterous manipulation.

Domenico Prattichizzo (M'95) received the M.S. degree in electronics engineering and the Ph.D. degree in robotics and automation from the University of Pisa, Pisa, Italy, in 1991 and 1995, respectively.

Since 2002, he has been an Associate Professor of robotics with the University of Siena, Siena, Italy. Since 2009, he has also been a Scientific Consultant with the Istituto Italiano di Tecnologia, Genova, Italy. In 1994, he was a Visiting Scientist with the Artificial Intelligence Laboratory, Massachusetts Institute of Technology, Cambridge, MA, USA. He was the Co-Editor of the books *Control Problems in Robotics* (Berlin, Germany: Springer, 2003), and *Multi-Point Physical Interaction with Real and Virtual Objects* (Berlin, Germany: Springer, 2005). He was the Guest Co-Editor of the Special Issue on "Robotics and Neuroscience" of the *Brain Research Bulletin* and "Visual Servoing" of *Mechatronics*, in 2008 and 2012, respectively. He was also a coauthor of the "Grasping" chapter of *Handbook of Robotics* (Berlin, Germany: Springer, 2008). He has authored more than 200 papers in robotics and automatic control. His research interests include haptics, grasping, visual servoing, mobile robotics, and geometric control.

Dr. Prattichizzo has been an Associate Editor-in-Chief of the IEEE TRANSACTIONS ON HAPTICS since 2007. From 2003 to 2007, he was an Associate Editor of the IEEE TRANSACTIONS ON ROBOTICS and the IEEE TRANSACTIONS ON CONTROL SYSTEMS TECHNOLOGY.